2 has about half the rate of the curve of Figure 1. In this connection it should be noted that the time t^* at which the maximum occurs when x and α are maintained constant (temperature and supersaturation are constant) is easily shown, via eq 12, to be given by

$$t^* = (x - 2)/\alpha \tag{14}$$

The agreement of the positions of maxima for the two curves thus indicates that both α and x are the same in the two cases, and the deviation in the least-squares-fitted values may be experimental errors resulting from the less complete signal averaging based on only 20 runs.

It should be possible to control the cloud chamber conditions so that single polymer nucleation occurs under different degrees of supersaturation (different values of M) but at the same temperature. Values of α obtained from such experiments could then be plotted vs. M to yield a straight line with slope, according to eq 5, equal to k_p. The intercept of this plot at $M = 0$ should then yield k_d. We have not yet accomplished this, but if we assume, to a first approximation, that k_d may be set equal to zero, then we can derive, from α alone, a value for k_p. A value so derived from the present data is $k_p \sim 3 \times 10^{-20}$ cm^3 molecule^{-1} s^{-1}. Values of k_p measured[4] for the free-radical chain reaction in liquid vinyl acetate are of the order of 5.4×10^{-19} cm^3 molecule^{-1} s^{-1}. Again there is nominal agreement.

In closing, it must be reemphasized that the device of assuming the existence of k_d can only be very approximate for these pulsed experiments. A growing free radical which diffuses out of the UV beam may continue to grow at different supersaturations and different temperatures as it wanders throughout the chamber and may then return to be counted within the optically defined volume of observation. An accurate assessment of the kinetics therefore requires knowledge of the time–position history of each counted polymer. Such information can only be made available through a detailed solution of the complicated boundary value problem involving both diffusion and reaction (and very complicated boundary conditions). In fact, since the critical degree of polymerization depends upon supersaturation, polymers may nucleate at different sizes at different elevations in the chamber. If these nucleation events occur at a position directly above the volume of observation, the drops which they produce will be counted. This is the reason why, in the measurements of the present paper, the count rate is taken to be *proportional* rather than *equal* to the rate of polymerization.

We have commenced work on the numerical solution of the above-mentioned boundary value problem. The solution is absolutely necessary if the cloud chamber technique is to be evolved into a precise method for measuring the kinetics of gas-phase polymerization.

Acknowledgment. This work was supported by NSF Grant No. ATM82-13871.

Registry No. Vinyl acetate, 108-05-4.

---

(4) Matheson, M. S.; Auer, E. E.; Bevilacqua, E. B.; Hart, E. J. *J. Am. Chem. Soc.* **1949**, *71*, 2610.

Collisional Deactivation of K(5^2P_J) by H_2. Identification of the Primary Quenching Channel

King C. Lin, Alan M. Schilowitz, and John R. Wiesenfeld*

Department of Chemistry, Cornell University, Baker Laboratory, Ithaca, New York 14853
(Received: April 4, 1984)

Pulsed photodissociation of KI at 193 nm was used as the source of K(5^2P_J) in a series of experimental studies of collisional deactivation. By comparison of the yield of ground-state K($4^2S_{1/2}$) in the presence and absence of H_2 and D_2, it was possible to demonstrate that chemical reaction plays no significant role in the deactivation process. Of the available quenching channels, that leading to the intermediate $5^2S_{1/2}$ and 3^2D_J states appears to dominate. The possible importance of near-resonant electronic-to-vibrational energy transfer is discussed and an application to the refinement of alkali metal lasers presented.

The term "superalkali" has been coined to describe alkali metal atoms in their electronically excited states.[1] The low ionization potential characteristic of alkali metals permits extensive delocalization of the single ns electron in the ground state during the course of collisions. The resulting high reactivity[2] (made manifest by large cross sections occasionally >1 nm^2) is also to be expected for the superalkalis as the unpaired electron lies even closer to the ionization potential. Whether such extraordinary reactivity is actually realized has primarily been a matter of conjecture for it is experimentally difficult to differentiate between chemical reaction of the superalkali, M*, and substrate, AB

$$M^* + AB \rightarrow MA + B$$

and the competing quenching process

$$M^* + AB \rightarrow M + AB$$

Further difficulties in assessing the relative importance of specific deactivation channels arise when multiple reactive and/or quenching pathways become available for the deactivation of a superalkali atom. This is often the case for alkali metals in excited states above the lowest-lying n^2P_J level.

Early experiments concerned with characterization of superalkali atom kinetics centered upon the measurement of total deactivation cross sections.[3,4] The use of variable-wavelength alkali halide photodissociation as a source of excited atoms permitted the production of superalkalis with a range of kinetic energies. Deactivating molecules could be grouped into four broad classes depending upon their electronic structure. Those molecules such as the alkanes with lowest unfilled orbitals of σ^* symmetry were generally inefficient in quenching M*. Those in which the lowest unoccupied orbital is π^*, but which cannot react exothermically to yield chemically distinct products, quench M* somewhat more efficiently. The most efficient deactivators provide

---

(1) Bersohn, R. In "Molecular Energy Transfer"; Levine, R., Jortner, J., Eds.; Wiley: New York, 1976; p 154. Barker, J. R.; Weston, R. E. *J. Chem. Phys.* **1976**, *65*, 1427. Bersohn, R. In "Alkali Halide Vapors: Structure, Spectra, and Reaction Dynamics"; Davidovits, P., McFadden, D. L., Eds.; Academic Press: New York, 1979; p 345.

(2) Davidovits, P.; In "Alkali Halide Vapors: Structure, Spectra, and Reaction Dynamics"; Davidovits, P., McFadden, D. L., Eds.; Academic Press: New York, 1979; p 331.

(3) Earl, B. L.; Herm, R. R. *Chem. Phys. Lett.* **1974**, *22*, 95.

(4) Earl, B. L.; Herm, R. R. *J. Chem. Phys.* **1974**, *60*, 4568.

0022-3654/84/2088-6670$01.50/0

exothermic reactive pathways for M*, the most electronegative substrates reacting most efficiently presumably as the result of electron-harpooning processes which also govern the reactions of ground-state alkali metal atoms with halogens and halides. It should be noted that these classifications were to a large degree inferred only from the measured total cross section for deactivation; specific channels for superalkali deactivation were not identified in these experiments.

More recently, laser excitation of specific electronic levels of superalkali atoms has been employed to provide more detailed information concerning the interaction of these chemically interesting species with deactivators. For example, it has been shown[5] that the deactivation of $Cs(7^2P_J)$ by H_2 does not proceed to any significant degree via the thermochemically accessible reactive pathway

$$Cs(7^2P_J) + H_2 \rightarrow CsH + H$$

in spite of the observation of CsH as "laser snow" during steady-state irradiation. Rather, production of diatomic CsH seems to involve a still-unresolved, multistep mechanism which is initiated by the formation of vibrationally excited H_2 or CsH_2 during the quenching of $Cs(7^2P_J)$; subsequent reaction involving either of the hypothesized intermediates with ground-state Cs may then yield CsH.[6]

The quenching of electronically excited alkali metals has been characterized under single-collision conditions in supersonic molecular beams. Observation of the product angular distributions in the quenching of $Na(3^2P)$ by H_2 and D_2 has permitted the identification of the detailed mechanism of these interactions;[7] approach on an attractive excited-state surface of NaH_2 is followed by a nonadiabatic hop to the repulsive ground-state surface. The resulting vibrational distributions are peaked at $v = 2$ and $v = 3$ for H_2 and D_2, respectively. Related studies of the $Na(3^2P_{3/2})$–N_2 interaction by observation of the effect of the orientation of reactants using polarized laser excitation[8] provide even greater insight into the dynamics of such quenching processes.

The deactivation by H_2 of electronically excited potassium in the second resonance state, $K(5^2P_J)$, may proceed by one or more of several available pathways. Chemical reaction to yield KH + H

$$K(5^2P_J) + H_2 \rightarrow KH + H \qquad (1)$$

is exothermic by 9.9 kcal/mol. Quenching of $K(5^2P_J)$ by H_2 can result in production of any of the lower electronic states of potassium, 3^2D_J, $5^2S_{1/2}$, 4^2P_J, or $4^2S_{1/2}$, via a complex sequence of collisional and radiative cascade processes (Figure 1). Concomitant vibrational excitation of the colliding hydrogen molecule following electronic quenching can also be expected. In the current work, the mechanism for $K(5^2P_J)$ deactivation by H_2 is elucidated by using time-resolved fluorescence and atomic absorption techniques. A specific quenching pathway, perhaps involving near-resonant electronic-vibrational energy transfer, is identified and the relative importance of chemical reaction discussed in terms of the potential surfaces available for the K–H_2 interaction.

Experimental Procedure

The experimental apparatus and techniques used were quite similar to those reported earlier.[9] In brief, samples of KI were photodissociated at 193 nm in a heated quartz fluorescence cell by using an ArF laser. This results in the formation of potassium atoms in the 5^2P_J state to the virtual exclusion of others. Condensation of the salt upon the cell windows was avoided by maintaining the central region of the cell at a temperature 50–80 K higher than of the KI reservoir which was usually in the vicinity of 725 K. The reservoir temperature was carefully controlled to ±1 K through the use of a proportional controller and monitored with a digital thermometer. Fluorescence signals associated with the transitions $K(5^2P_J) \rightarrow K(4^2S_{1/2}) + h\nu$ (404 nm) and $K(4^2P_{3/2}) \rightarrow K(4^2S_{1/2}) + h\nu$ (767 nm) were monitored photoelectrically by using either narrow-band filters or a small, high-efficiency double monochromator for wavelength discrimination. The emission transients were recorded by using a boxcar averager (PAR 162/165) operated in the A/B mode in order to account for shot-to-shot intensity fluctuations in the photolysis laser output which was monitored by using a fast photodiode. Recorded transients were stored in a laboratory microcomputer and transferred to a minicomputer for complete kinetic analysis.

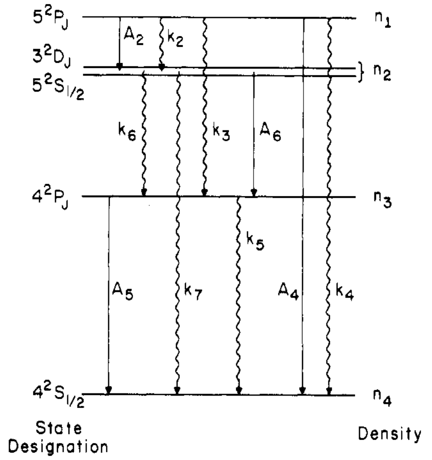

Figure 1. Lower electronic states of atomic potassium showing both the radiative cascade and collisional processes which are characterized by the Einstein coefficients, A_i, and rate constants, k_i, respectively. The 3^2D_J and $5^2S_{1/2}$ states lie so close in energy as to be kinetically and spectroscopically indistinguishable in the current experiments.

In a separate apparatus, the total yield of ground-state potassium, $K(4^2S_{1/2})$, following deactivation of $K(5^2P_J)$ by H_2 was measured. Samples of KI were placed in a cylindrical quartz cell (25 mm o.d. × 150 mm long). As described previously,[10] the salt was photolyzed with an ArF laser directed along the axis of the cell. Coincident with the laser beam was the collimated output of a potassium hollow cathode lamp. The density of $K(4^2S_{1/2})$ in the cell was monitored by observing the absorption of the atomic resonance radiation at 767 nm as a function of time following the photodissociating laser pulse. Comparison of the magnitude of the observed absorption transient determined by time-resolved atomic absorption spectroscopy in the presence and absence of deactivating gas yields a direct estimate of the fraction of photolytically produced, electronically excited potassium atoms in the ^5P_J state which was collisionally removed by chemical reaction with the deactivator. As will be demonstrated in the next section, detailed quantitative treatments of the absorption transients are not necessary because the magnitude of the observed signals are, within experimental error, identical regardless of the presence of deactivating gases studied in the present work.

Finally, due regard was paid to the potential role of metal ions which are easily produced following energy pooling collisions of the type[11]

$$K^* + K^* \rightarrow K_2^+ + e^-$$

direct multiphoton excitation of KI, or direct ionization of $K(5^2P_J)$ by the 193-nm actinic radiation. Samples of KI were placed in a small quartz cell similar in construction to the fluorescence cell but containing nichrome electrodes. These electrodes were then biased at 200 V and the current flow was measured following KI photodissociation under conditions similar to those of the fluorescence experiments. The magnitude of the currents observed

---

[5] Sayer, B.; Ferray, M.; Lozingot, J.; Berlande, J. *J. Chem. Phys.* **1981**, *75*, 3894.

[6] Visticot, J. P.; Ferray, M.; Lozingot, J.; Sayer, B. *J. Chem. Phys.* **1983**, *79*, 2839.

[7] Reiland, W.; Tittes, V.; Hertel, I. V. *Phys. Rev. Lett.* **1982**, *48*, 1389.

[8] Reiland, W.; Jamieson, G.; Tittes, V.; Hertel, I. V. *Z. Phys. A* **1982**, *307*, 51.

[9] Schilowitz, A. M.; Wiesenfeld, J. R. *J. Phys. Chem.* **1983**, *87*, 2194.

[10] Schilowitz, A. M.; Wiesenfeld, J. R.; Young, R. H. *J. Phys. Chem.* **1982**, *86*, 692.

[11] Allegrini, M.; Gozzini, S.; Long, I.; Savino, P.; Bicchi, P. *Nuovo Cimento Soc. Ital. Fis., D* **1982**, *1D*, 49.

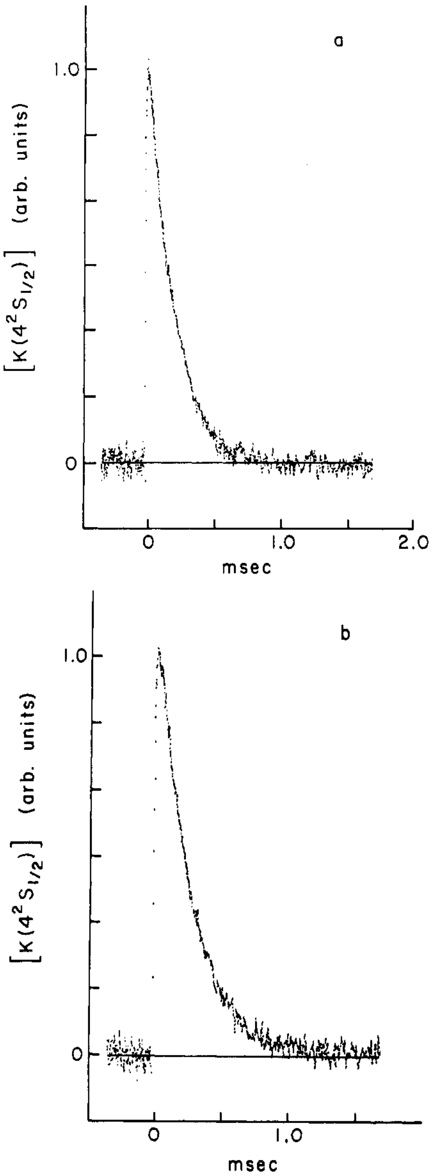

Figure 2. Temporal profile of $[K(4^2S_{1/2})]$ obtained from the observed attenutation of $K(4^2P_{1/2} \leftarrow 4^2S_{1/2})$ resonance radiation from a hollow cathode lamp following photodissociation of KI ($p \sim 1$ mtorr) (a) in the absence of H_2 and (b) at $P_{H_2} = 97$ torr. The total pressure was maintained at 107 torr with Ar to minimize possible changes in the nominal detection sensitivity due to pressure broadening. The observed signal maximum corresponds to a $K(5^2P_J)$ density of ca. 10^{12} cm^{-3}.

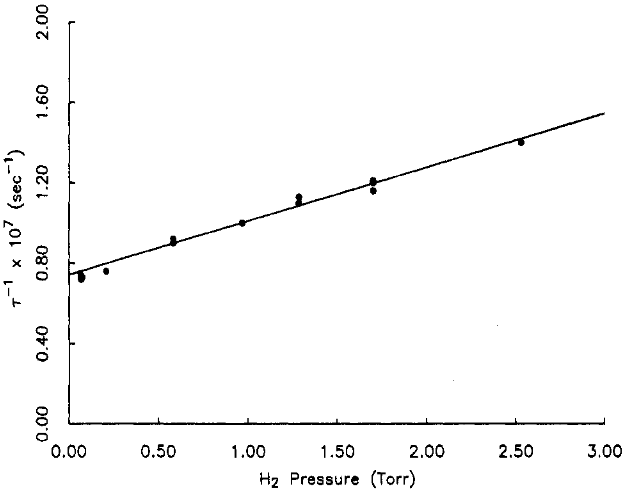

Figure 3. Pressure dependence of characteristic time constant for deactivation of $K(5^2P_J)$ in the presence of hydrogen.

suggest that the concentration of ions and electrons under these conditions never exceeds 5×10^8 cm^{-3}; it is thus concluded that such processes as radiative recombination, electron quenching, etc., play no significant role in the present experiments.

The experimental studies reported here were primarily carried out with H_2 (Matheson, 99.9995%) which was passed through a liquid-N_2 trap immediately prior to use. Some experiments were carried out with D_2; except as noted in the text, the results obtained were identical with those observed for H_2.

Results

The relative contribution of chemical reaction to the overall collisional deactivation of $K(5^2P_J)$ by H_2 can be directly assessed by monitoring the yield of ground-state potassium following ArF laser photolysis of KI in the presence of a large pressure of hydrogen. As the optical lifetime of $K(5^2P_J)$ is ca. 140 ns[12] and the cross section for $K(5^2P_J)$ deactivation by H_2, σ_{H_2}, is reported as either 1.2[6] or 6[13] nm^2, over 98% of the initially excited potassium atoms will be collisionally deactivated when $1/\tau < 0.02\,\sigma_{H_2} n_{H_2} \bar{v}$, a condition met at $P_{H_2} > 100$ torr, even at the lower reported value of σ_{H_2}. Here, $\bar{v}$ represents the mean thermal collision velocity.

The attenuation of resonance radiation by $K(4^2S_{1/2})$ following KI photodissociation is seen (Figure 2) not to depend on the presence of H_2 or D_2 at pressures as high as 94 torr. It may thus be concluded that chemical reaction of $K(5^2P_J)$ with H_2 does not contribute significantly to the overall deactivation rate. On the basis of the observed signal quality, the relative contribution of chemical reaction may be estimated, $k_1/k_{H_2} < 0.01$. Here, k_{H_2} represents the total rate of $K(5^2P_J)$ deactivation by H_2 by both reaction and quenching channels discussed below.

A direct determination of k_{H_2} is afforded in the current study by observation of the observed lifetime of $K(5^2P_J) \rightarrow K(4^2S_{1/2})$ fluorescence at 404 nm as a function of quenching gas pressure. The integrated rate expression

$$[K(5^2P_J)]_t = [K(5^2P_J)]_0 \exp(-t/\tau)$$

can be related to the quenching rate by $\tau^{-1} = \tau_{optical}^{-1} + k_{H_2}[H_2]$. The variation in τ^{-1} as a function of P_{H_2} (Figure 3) yields estimates for both k_{H_2} (791 K) = $(2.2 \pm 0.1) \times 10^{-10}$ cm^3 s^{-1} and $\tau_{optical} = 139 \pm 1$ ns. The latter value is in excellent agreement with an earlier result[12] obtained by using the optical zero-crossing method, 140.8 ± 1.0 ns. The rate constant is in sensible accord with that derived from steady-state photolysis measurements[4] carried out at 893 K, 3.8×10^{-10} cm^3 s^{-1}, but is substantially smaller than that measured at 1900 K in a flame.[13] The value of k_{H_2} measured here was not affected by the addition of $P_{Ar} = 500$ torr, thereby demonstrating that translational disequilibrium was of no noticeable import in the current studies.

Having established that quenching plays an overwhelmingly dominant role in the exceptionally efficient deactivation of $K(5^2P_J)$ by H_2 we must assess the relative contributions of the various quenching pathways. These include the following:

$$K(5^2P_J) + H_2 \rightarrow K(5^2S_{1/2},3^2D_J) + H_2 \tag{2}$$

$$\rightarrow K(4^2P_J) + H_2 \tag{3}$$

$$\rightarrow K(4^2S_{1/2}) + H_2 \tag{4}$$

A qualitative impression of the relative importance of these quenching processes can be immediately gleaned from the observation that the intensity of the $K(4^2P_{3/2} \rightarrow 4^2S_{1/2})$ emission following 193-nm photolysis of KI increases upon addition of H_2 (Figure 4). Were reaction 4 to dominate the deactivation of $K(5^2P_J)$ by H_2, the 767-nm emission intensity could only decrease upon H_2 addition because the direct removal of the 5^2P_J level to

---

(12) Schmieder, R. W.; Lurio, A.; Happer, W. *Phys. Rev.* **1968**, *173*, 76.

(13) Hooymayers, H. P.; Lijnse, P. J. *J. Quant. Spectrosc. Radiat. Transfer* **1969**, *9*, 995.

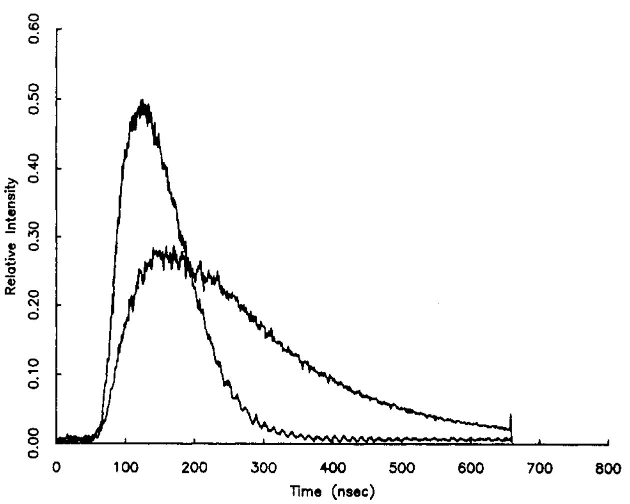

Figure 4. Temporal dependence of the 767-nm emission K($4^2P_{1/2} \rightarrow 4^2S_{1/2}$) at $P_{H_2} = 0$ (lower intensity, longer-lived) and $P_{H_2} = 5$ torr (more sharply peaked and shorter-lived).

TABLE I: Kinetic Parameters Describing the Collisional Quenching of K(5^2P_J) by H_2 in Eq 5[a]

parameter	value
α_1	$-\{l/(m-p) + n/(m-q)\}$
α_2	$l/(m-p)$
α_3	$n/(m-q)$
τ_1	$(A_5 + k_5[H_2])^{-1}$
τ_2	$(A_2 + A_4 + (k_2 + k_3 + k_4)[H_2])^{-1}$
τ_3	$(A_6 + (k_6 + k_7)[H_2])^{-1}$

[a] $l = k_3[H_2] + (A_6 + k_6[H_2])\{r/(q-p)\}$. $m = A_5 + k_5[H_2]$. $n = -(A_6 + k_6[H_2])\{r/(q-p)\}$. $p = \tau_{optical}^{-1} + k_{H_2}[H_2]$. $q = A_6 + (k_6 + k_7)[H_2]$. $r = A_2 + k_2[H_2]$.

the ground state would deplete the concentration of the $4^2P_{3/2}$ state which can only be formed (in the absence of collisional processes 2 and/or 3) via a radiative cascade through the intermediate 3^2D_J and $5^2S_{1/2}$ levels.

Not so readily ascertained by simple inspection of the far-red emission transient profile is the relative contribution of reactions 2 and 3. Here, quantitative modeling of the radiative and collisional processes described in Figure 1 is required. The temporal variation in the density of potassium in the $4^2P_{3/2}$ excited state can be expressed in the form (see Appendix)

$$[K(4^2P_{3/2})]_t = \alpha_1 \exp(-t/\tau_1) + \alpha_2 \exp(-t/\tau_2) + \alpha_3 \exp(-t/\tau_3) \quad (5)$$

where the values of the characteristic parameters, α_i, and time constants, τ_i, are presented in Table I. Similar expressions may be derived for the other potassium electronic states, although they will not be presented here. Limited observation of the $4^2P_{1/2} \rightarrow 4^2S_{1/2}$ emission at 770 nm suggested behavior similar to that observed at 767 nm. For the succeeding discussion, the radiative and collisional processes involving the other spin–orbit $J = {}^1/_2$ level of the lowest resonance state are ignored because it appears under the present conditions to be in thermal equilibrium with the higher $J = {}^3/_2$ level.

Were the attainable signal quality sufficiently high, it should in principle be possible to derive the kinetic parameters directly from a least-squares fit of eq 5 to the data. In the present case, however, this would require exceptionally high signal-to-noise ratios in order to minimize the inevitable (but often not reported) correlation of parameters derived from such a procedure.[14] As an alternative, we used expression 5 to predict the excited potassium atom density $[K(4^2P_{3/2})]_{t_{max}}$ at $t = t_{max}(H_2{=}0)$, the time at which the fluorescence signal peaked when no H_2 was added to the photolysis cell, over the range of hydrogen pressures used in the present study. The value of $[K(4^2P_{3/2})]_t$ is taken here as being proportional to the output signal of the boxcar averager; i.e., the gate width of the boxcar is assumed infinitesimal with respect to the variation of the emission signal. The modeling results were tested by convoluting exponential gate functions as wide as 15 ns with the theoretical profiles; the minor changes noted have no impact upon the interpretation of the experimental observations. Deactivation of K(5^2D_J) by D_2 yielded results which were experimentally indistinguishable from those obtained with H_2.

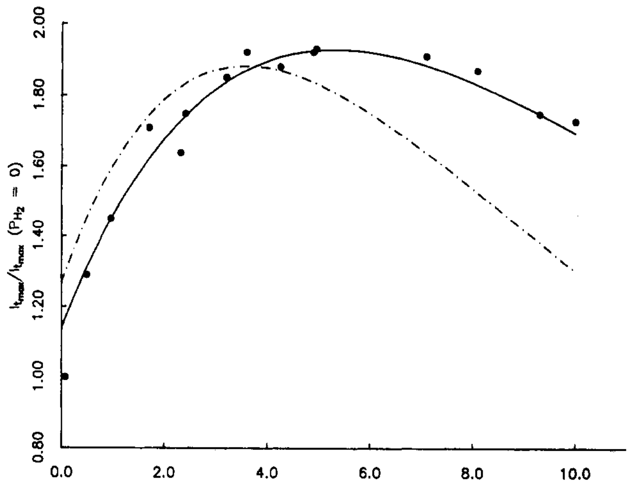

Figure 5. Pressure dependence of the intensity of 767-nm emission (measured at t_{max} for $P_{H_2} = 0$) as a function of hydrogen pressure. The experimental points are better fit by the calculated values for $k_3 = k_4 = 0$, $k_2 = k_{H_2}$ (solid line) than those for $k_2 = k_4 = 0$, $k_3 = k_{H_2}$ (dot–dash line).

Two extreme cases may be profitably considered here, namely $k_2 = 0$, $k_3 = k_{H_2}$ and $k_2 = k_{H_2}$, $k_3 = 0$. The predicted variation in $[K(4^2P_{3/2})]_{t_{max}}$ for these two sets of critical parameters is compared to the experimental result in Figure 5. Of the two cases, the variation in potassium atom emission intensity at 767 nm with hydrogen pressure is clearly better fitted by a mechanism in which the quenching of K(5^2P_J) proceeds initially via reaction 2 to yield potassium atoms in the 3^2D_J or $5^2S_{1/2}$ states which are kinetically indistinguishable here. The initial increase in $[K(4^2P_{3/2})]_{t_{max}}$ with increasing hydrogen pressure is related to the competition of the quenching channel 2 followed by relatively rapid production of K($4^2P_{3/2}$) via optical relaxation of the intermediate states as well as further collisional quenching

$$K(3^2D_J,5^2S_{1/2}) + H_2 \rightarrow K(4^2P_{3/2}) + H_2 \quad (6)$$

Upon continued addition of H_2, the value of $[K(4^2P_{3/2})]_{t_{max}}$ is expected to decrease because the time scale of the quenching becomes shorter so that the observed emission at t_{max}, which is held fixed, becomes less. Were quenching process 3 to dominate, $[K(4^2P_{3/2})]_{t_{max}}$ would increase more rapidly at low P_{H_2} than is actually observed in these experiments. In effect, the intermediacy of the 3^2D_J and $5^2S_{1/2}$ states leads to a "delay" in the observed variations of the emission transient intensity at 767 nm, a phenomenon reflected in the dependence of $[K(4^2P_{3/2})]_{t_{max}}$ upon hydrogen pressure.

Relatively little information concerning the collisional quenching of the intermediate states by H_2 can be gleaned from the present experiments, for their optical lifetimes are so short[15] ($\tau_{3D} = 38$ ns, $\tau_{5S} = 43$ ns) that addition of H_2 at the pressures employed here has only a minor effect on the rate of their removal. Nonetheless, the kinetic data and model calculations suggest that the apparent quenching of the intermediate states (lumped together because they cannot be resolved in the present scheme) does not exceed $k_6 = 10^{-10}$ cm^3 s^{-1}, a result which seems reasonable in view

---

(14) Carrington, T. *Int. J. Chem. Kinet.* **1982**, *14*, 517.

(15) Wiese, W. L.; Smith, M. W.; Miles, B. M. *Natl. Stand. Ref. Data Ser.* (*U.S., Natl. Bur. Stand.*) **1969**, *NSRD-NBS 2*.

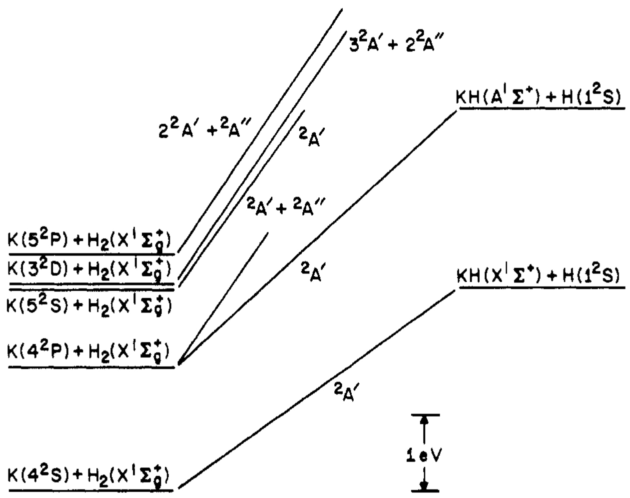

Figure 6. Adiabatic correlation diagram for the reaction $K + H_2 \rightarrow KH + H$.

of the known rate[4] of $K(4^2P_J)$ deactivation by H_2, 9.45×10^{-11} $cm^3\ s^{-1}$.

Discussion

The chemistry of superalkali atoms following collisional interactions with atoms and small molecules has been intensely studied. It would appear, however, that nowhere has the relative importance of chemical reaction with respect to physical quenching been directly assessed for a case where multiple deactivation pathways are available. This is in part due to the use of the alkali metal itself as a source (following narrow-band laser excitation) of the superalkali. In the present study, the use of KI photolysis as a source of excited atoms permits the unambiguous observation of the yield of ground-state potassium atoms, $K(4^2S_{1/2})$, following the deactivation of $K(5^2P_J)$. The magnitude of the resonance absorption signal observed at relatively long time (>1 μs) following KI photolysis in the absence of H_2 reflects the yield of $K(5^2P_J)$ because any excited potassium atoms formed in the photodissociation of KI will relax to the ground state by radiative processes only. Addition of H_2 at sufficiently high pressure will ensure that any such excited atoms formed by photolysis will be deactivated collisionally. That no change in the absorption signal could be discerned immediately suggests that reaction 1 plays no significant role in the deactivation of $K(5^2P_J)$ by H_2.

The lack of reactivity of a superalkali with H_2 has previously been inferred from CW laser excitation studies of $Cs(7^2P_J)$ interactions with H_2.[5] Although the formation of CsH as laser snow does occur, it would appear that the actual bimolecular step leading to reaction involves not the excited cesium atoms, but rather vibrationally excited H_2 or CsH_2, which presumably arise from the $Cs(7^2P_J)$ deactivation. Recently reported studies suggest[6] that the mechanism of this relaxation is in some doubt, but the analogue of reaction 1 certainly does not appear to be responsible for the observed reaction products. It should be noted that formation of solid KH would not in any case be expected under the current experimental conditions. Use of pulsed laser excitation would prevent sufficient accumulation of whatever intermediate is required to actually yield KH in a multistep mechanism.

Examination of a state correlation diagram[16] (Figure 6) reveals that no adiabatic pathway conservative of electronic orbital angular momentum connects $K(5^2P_J) + H_2$ with $KH(X^1\Sigma^+) + H(^2S_{1/2})$. This, in turn, would suggest that a nonadiabatic transition would be required in order that a bimolecular chemical reaction occur. Such a process would then need to proceed rapidly with respect to quenching which by its essence must also be nonadiabatic. This appears not to be the case during the $K(5^2P_J)/H_2$ interaction.

It is interesting that the deactivation of $K(5^2P_J)$ by H_2 occurs primarily via process 2. This observation may be compared to similar effects noted in the quenching of such highly excited species as $Hg(6^3P_2)$[17] where intramultiplet relaxation is far more efficient than is quenching via the channel leading to direct production of the ground-state atom, the latter involving a discrepancy of many electronvolts between the electronic quantum of the atom and the vibrational spacing of the deactivator. In the case of $K(5^2P_J)$, the magnitude of the electronic energy lost following deactivation to the 3^5D_J, $5^2S_{1/2}$, and $4^2P_{3/2}$ states is on the order of 3200, 3700, and 11 700 cm^{-1}, respectively.

Whether a specific mechanism involving near-resonant E–V energy transfer from $K(5^2P_J)$ to H_2 can account for the large cross section of reaction 2 must, at present, remain a matter of speculation. It is probably significant to note, however, that the deactivation of $K(5^2P_J)$ by D_2, for which the vibrational quantum is only 3000 cm^{-1}, appears to proceed by a mechanism similar to that for H_2, which has a vibrational spacing of 3840 cm^{-1}. One might hypothesize that, were such near-resonant effects significant, then different quenching pathways would dominate for the two hydrogen isotopes, i.e.

$$K(5^2P_J) + H_2(v''=0) \rightarrow K(5^2S_{1/2}) + H_2(v''=1) - \sim 140\ cm^{-1}$$

$$K(5^2P_J) + D_2(v''=0) \rightarrow K(3^2D_J) + D_2(v''=1) + \sim 200\ cm^{-1}$$

The present experimental technique does not permit discrimination of these two mechanisms. Furthermore, it is not clear how a long-range interaction such as that characterizing the collision of an excited superalkali atom with H_2 would result in a highly specific near-resonant transfer of a relatively small fraction of the total available electronic energy to vibration in the collision partner. After all, the rate of $K(4^2P_J)$ quenching by H_2 which must involve a long-range interaction and presumably (by analogy with the known propensity[7] for multiquantum vibrational excitation in $Na(3^2P_J) + H_2$) efficient transfer of ~17 000 cm^{-1} into vibration occurs with a rate constant only a factor of 2 smaller than $k_2 = k_{H_2}$. It seems clear that our understanding of relaxation processes governing the collisional behavior of highly excited atomic states in gases is far from complete.

It should be possible to probe the time dependence of the population ratios, $[K(5^2S_{1/2})]/[K(4^2P_J)]$ and $[K(3^2D_J)]/[K(4^2P_J)]$, by monitoring the gain achieved on the near-infrared lasing transitions[18] $5^2S_{1/2} \rightarrow 4^2P_J$ ($\lambda \sim 1.25$ μm) and $3^2D_J \rightarrow 4^2P_J$ ($\lambda \sim 1.17$ μm) with different additions of quenching gases. Indeed, it seems not improbable that the use of specific additives will actually enhance the performance of such lasers by selectively populating upper lasing levels without significantly changing that of the lower one. Such an approach to the design of electronic transition lasers has not to date been explored, but could lead to a broader selection of high-energy devices operating in the near-infrared and visible regions of the spectrum.

Acknowledgment. This work was supported by the U.S. Air Force Office of Scientific Research and the National Science Foundation.

Appendix

The kinetic model describing the observed behavior of electronically excited potassium atoms following KI photolysis at 193 nm may be derived in the following manner. We assume that such photolysis leads exclusively to the formation of $K(5^2P_J)$ and no other state of potassium as confirmed in previous work from this laboratory. The states shown in Figure 1 are treated in terms of a four-level model; because the 3^2D_J and $5^2S_{1/2}$ states lie in such close proximity and could at best only be detected in infrared emission, they are experimentally indistinguishable here and are considered as one level. Similarly, individual spin–orbit levels are unresolved kinetically. The reactive channel 1 and the formation of ions via energy pooling processes are also ignored as they appear not to be of any importance in the present system. Only collisional

---

(16) Donovan, R. J.; Husain, D. *Chem. Rev.* **1970**, *70*, 489.

(17) Pitre, J.; Hammond, K.; Krause, L. *Phys. Rev. A* **1972**, *6*, 2101.

(18) Ehrlich, D. J.; Osgood, Jr., R. M. *Appl. Phys. Lett.* **1979**, *34*, 655.

J. Phys. Chem. **1984**, *88*, 6675–6680 **6675**

events involving H_2 need be considered because the pressure of KI is only ~1 mtorr or less.

The rate equations describing the model kinetics are

$$\mathrm{d}n_1/\mathrm{d}t = -(A_2 + A_4 + \{k_2 + k_4 + k_3\}[\mathrm{H_2}])n_1 \quad \text{(A1)}$$

$$\mathrm{d}n_2/\mathrm{d}t = -(A_6 + \{k_6 + k_7\}[\mathrm{H_2}])n_2 + (A_2 + k_2[\mathrm{H_2}])n_1 \quad \text{(A2)}$$

$$\mathrm{d}n_3/\mathrm{d}t = -(A_5 + k_5[\mathrm{H_2}])n_3 + k_3[\mathrm{H_2}]n_1 + (A_6 + k_6[\mathrm{H_2}])n_2 \quad \text{(A3)}$$

$$\mathrm{d}n_4/\mathrm{d}t = (A_4 + k_4[\mathrm{H_2}])n_1 + (A_5 + k_5[\mathrm{H_2}])n_3 + k_7[\mathrm{H_2}]n_2 \quad \text{(A4)}$$

with the conservation of mass demanding $n_1 + n_2 + n_3 + n_4 = n_1$ $(t = 0)$, which for the sake of convenience is here set equal to unity. The densities, n_i, spontaneous emission coefficients, A_i, and rate coefficients, k_i, are presented in Figure 1.

Solution of eq A1 yields the time dependence of the 5^2P_J state

$$n_1(t) = \exp(-(A_2 + A_4 + \{k_2 + k_3 + k_4\}[\mathrm{H_2}])t) \quad \text{(A5)}$$

As expected, this state decays with a characteristic rate equal to the sum of the rates of all of the processes leading from it. Initially, $n_2 = n_3 = n_4 = 0$. Substitution of eq A5 into eq A1 yields the solution for the time dependence of the intermediate state ($5^2S_{1/2} + 3^2D_J$) density

$$n_2(t) = r/(q - p)\exp(-pt) - r/(q - p)\exp(-qt) \quad \text{(A6)}$$

where $r = A_2 + k_2[\mathrm{H_2}]$, $q = A_6 + (k_6 + k_7)[\mathrm{H_2}]$, and $p = \tau_{\mathrm{optical}}^{-1} + k_{\mathrm{H_2}}[\mathrm{H_2}]$. Further substitution of eq A5 and A6 into eq A3 yields the desired time dependence of the 4^2P_J state which is presented in the text as eq 5 and the parameters for which are given in Table I.

Values for the spontaneous emission rates[15] are as follows: $A_2 = 6.1 \times 10^6$, $A_4 = 1.24 \times 10^6$, $A_5 = 3.85 \times 10^7$, and $A_6 = 4..7 \times 10^7$ s^{-1}. The value of k_5 is taken to be 9.45×10^{-11} cm^3 s^{-1} while that of k_6 is 5×10^{-11}.

Registry No. KI, 7681-11-0; K, 7440-09-7; H_2, 1333-74-0; deuterium, 7782-39-0.

Kinetics and Equilibria in the System Br + $CH_3OOH \rightleftharpoons$ HBr + CH_3OO. An Upper Limit for the Heat of Formation of the Methylperoxy Radical

Osamu Kondo and Sidney W. Benson*

Loker Hydrocarbon Research Institute, Department of Chemistry, University of Southern California, University Park MC-1661, Los Angeles, California 90089 *(Received: May 16, 1984; In Final Form: August 1, 1984)*

Very low pressure reactor technique (VLPR) is used to study the reaction Br + $CH_3OOH \rightleftharpoons$ HBr + $CH_3O_2\cdot$ (1) at 298–333 K. The *A* factor for the reaction is estimated on the basis of the tight transition state model and is combined with the measured k_1 to give the Arrhenius equation: $\log (k_1/(\mathrm{L/mol\ s})) = (9.2 \pm 0.3) - (3.2 \pm 0.4)/\theta$, where $\theta = 2.303RT$ kcal/mol. A lower limit of K_1 is measured at 333 K. Using an estimated $\Delta S_1° = 3.6 \pm 1.1$ eu, we then place the upper limits to DH°(CH_3OO–H) < 89.6 kcal/mol, $\Delta H_f°(CH_3OO) < 6.6$ kcal/mol. Other pathways for reaction 1 are shown to be unimportant and the secondary reaction Br + $CH_3OO \rightarrow$ HBr + CH_2OO (the Criegee zwitterion) is shown to also be unimportant. From data on H_2O_2, *t*-BuO_2H and arguments about the probable upper limit for K_1 we obtain DH°(CH_3O_2–H) = 88.5 ± 0.5 kcal/mol as a best value.

Introduction

Methylperoxy radical (CH_3OO) is known to play an important role in combustion and in the upper atmosphere.[1] For instance, it is produced by the photochemical oxidation of methane and its subsequent reaction with ambient NO producing NO_2 is a key step in the formation of ozone in the troposphere.[2,20] One of the important radical loss processes both in combustion and in atmospheric chemistry is the reation with HO_2 forming methyl hydroperoxide:

$$\mathrm{CH_3OO + HO_2 \rightarrow CH_3OOH + O_2}$$

Recently, the possible fate of CH_3OOH thus formed has been discussed.[3]

Despite the important roles that CH_3OO plays in all oxidation processes,[4] very few attempts have been made to fix its thermochemistry experimentally. In order to derive the heat of formation $\Delta H_f°(CH_3OO)$, Benzon[5] had first assumed that the O–H bond strength in the hydroperoxide is equal to that of hydrogen peroxide, i.e., DH°(CH_3OO–H) = DH°(HO_2–H) = 89.6 ± 2 kcal/mol based on $\Delta H_f°(HO_2) = 5.0 \pm 2$ kcal/mol measured by Foner and Hudson.[6] The validity of this assumption was given further support by Nangia and Benson[7] in their analyses of the decomposition kinetics of R_2O_3 and R_2O_4 both in the gas phase (R = SF_5) and in solution (R = *t*–Bu). Recent renewal of interest in HO_2 chemistry, however, has prompted the remeasurement of $\Delta H_f°(HO_2)$ and a value of $\Delta H_f°(HO_2) = 3.5^{+1.0}_{-0.5}$ kcal/mol is currently recommended by Shum and Benson in their review article.[8] With $\Delta H_f°_{298}(CH_3OOH) = -30.9 \pm 1.0$ and DH°$_{298}$(HO_2–H) = 88.2 ± 0.4 kcal/mol = DH°$_{298}$(CH_3O_2–H), this gives $\Delta H_f°_{298}(CH_3O_2) = 5.2 \pm 1.1$ kcal/mol. Since $\Delta H_f°(CH_3OO)$ will provide an important data base for the group additivity scheme of the various polyoxide series,[9] independent measurements of this value are highly desirable.

Recently, Khachatryan et al.[10] have studied the equilibrium reaction

$$\mathrm{CH_3 + O_2 \rightleftharpoons CH_3OO}$$

in the low-temperature oxidation of methane by the ESR detection of CH_3OO radical and obtained a value of $\Delta H_f°(CH_3OO)$ = 2.8

---

(1) See for example: Baulch, D. L.; Cox, R. A.; Hampson, R. F., Jr., Kerr, J. A.; Troe, J.; Watson, R. T. *J. Phys. Chem. Ref. Data* **1982**, *11*, 327.

(2) Okabe, H. "Photochemistry of Small Molecules"; Wiley: New York, 1978.

(3) Niki, H.; Maker, P. D.; Savage, C. M.; Breitenbach, L. P. *J. Phys. Chem.* **1983**, *87*, 2190. Molina, M. J.; Arguello, G. *Geophys. Res. Lett.* **1979**, *6*, 953.

(4) Benson, S. W.; Nangia, P. S. *Acc. Chem. Res.* **1979**, *12*, 223.

(5) Benson, S. W. *J. Am. Chem. Soc.* **1965**, *87*, 972.

(6) Foner, S. N.; Hudson, R. L. *J. Chem. Phys.* **1962**, *36*, 2681.

(7) Nangia, P. S.; Benson, S. W. *J. Phys. Chem.* **1979**, *83*, 1138.

(8) Shum, L. G. S.; Benson, S. W. *J. Phys. Chem.* **1983**, *87*, 3479.

(9) Benson, S. W.; Shaw, R. "Organic Peroxides"; Wiley: New York, 1970; Vol. 1, 105.

(10) Khachatryan, L. A.; Niazyan, O. M.; Mantashyan, A. A.; Vedeneev, V. I.; Teitel'Boim, M. S. *Int. J. Chem. Kinet.* **1982**, *14*, 1231.

0022-3654/84/2088-6675$01.50/0